JOURNAL OF MATERIALS SCIENCE 28 (1993) 6381–6391

Fracture behaviour of model toughened composites under Mode I and Mode II delaminations

H.-J. SUE, R. E. JONES, E. I. GARCIA-MEITIN
Dow Chemical USA, Polymer Materials Science Group, B-1470, Texas Polymer Center, Freeport, TX 77541, USA

The fracture behaviour of two toughened epoxy composite systems was investigated using various microscopy techniques. The Mode I delamination fracture toughness, G_{IC}, Mode II delamination fracture toughness; G_{IIC}, and compression after impact (CAI) strength of these model composite systems were also measured. Under Mode I fracture, it was found that these composites exhibit nearly identical toughening mechanisms to those of the rubber-modified neat resins. The composites differ primarily in having smaller damage zones than the neat resin equivalents. Under Mode II fracture, the typical hackles were found to initiate from inside the resin-rich interlaminar region due to the presence of the toughener particles. The CAI strength, based on the present study as well as the work conducted by others, appeared to be related to, but not necessarily strongly dependent on, the interlaminar G_{IC} and G_{IIC}, the thickness of the interlaminar resin-rich region, and the type of the interlaminar toughener particles. Approaches for improving the G_{IC}, G_{IIC}, and CAI strength of high-performance toughened composites are discussed.

1. Introduction

The ever-increasing demand for high-performance composites for aerospace applications has driven tremendous research effort in understanding how the mechanical properties of a composite can be improved [1–14]. It has been found that both the morphology and the composite micro-architecture, such as the resin phase morphology, the locations in which the toughener particles reside, and the thickness of the interlaminar resin-rich region, are critical in effecting toughening of high-performance composites [1, 3, 6, 11, 13, 14]. The reproducibility of the mechanical properties of the composite is also found to depend greatly on how well the resin phase morphology is controlled [2, 6, 11, 14]. In spite of these findings, several questions concerning how to improve the compression after impact (CAI) strength, which is among the most important mechanical properties for high-performance composites, still remain, such as:

1. Do Mode I, G_{IC}, and Mode II, G_{IIC}, interlaminar fracture toughnesses strongly influence the CAI strength of the composite?
2. How do the large interlaminar elastomeric particles influence the CAI strength of the interleaved composites?
3. Is the type of interleaving particles important?
4. Is intralaminar toughening important?

In order to clarify the relationship between the composite mechanical performance and fracture micromechanisms, unambiguous studies of the fracture behaviour of model composites, i.e. study of the toughening mechanisms and micromechanics under specific and analysable loading conditions, are required. This will, in turn, help elucidate how the CAI strength of high-performance composites can be improved.

Laminated continuous fibre composites are highly anisotropic and are micromechanically complex. The traditional approaches using rubber particles for toughening thermosets usually do not produce the expected toughness improvements in the composites [2–5]. The rubber modification approach usually causes stiffness, thermal stability, glass transition temperature and composite processability reductions. Furthermore, rubber modification in composites sometimes reduces G_{IC} [2] and often reduces G_{IIC} [5, 6]. As a result, the CAI performance, which has empirically correlated well with both G_{IC} and G_{IIC} [5–10], is not significantly improved after rubber modification. Hence, significant effort has been focused on improving CAI strength through either thermoplastic modification or micro-architectural design of the composites [6, 11–14].

The concept of using thermoplastic modification in composites is quite similar to the rigid–rigid polymer toughening concept [15–18], which utilizes an engineering polymer to toughen another engineering polymer, in high-performance thermoplastics and thermosets applications. However, this approach, depending on the type of thermoplastic and how it is incorporated into the composite, does not always produce an acceptable toughening effect and consistent mechanical properties [11, 13, 14]. Therefore, research is also focused on the micro-architectural

0022–2461

design of the composites to improve the CAI strength. In micro-architectural design of high-performance composites, it has been widely speculated that the thickness of the resin-rich interlaminar region gives rise to the impressive improvement of the CAI strength. Consequently, it is thought that any interlaminar interleaving approach that can result in a controlled, thick, resin-rich region in the laminate should greatly improve the CAI strength of the composite. The type of large interleaving particles which should be utilized is believed to be much less important. This conjecture, even though well-supported from the published data, still needs to be confirmed [6, 11–14].

As pointed out earlier, for unidirectional fibre composite systems, under Mode I fracture, rubber modification appears to produce less than the expected toughening effect and may sometimes give a lower G_{IC} than an unmodified counterpart [2]. One of our earlier studies suggests that ineffective rubber toughening may result from poor dispersion of the rubber particles in the composite matrix [19]. Also, ineffective toughening may simply be due to the hindrance of the fibre phase, which limit the growth of the crack-tip damage zone [3, 20].

When the composite experiences Mode II shear, it has been repeatedly shown that rubber modification cause a reduction in G_{IIC} values as compared to the unmodified composites [6, 21]. However, it is still unclear how the rubber-modified composite fails under Mode II fracture. More specifically, the role the rubber particles play during the fracture process, under both Mode I and Mode II loading, is not understood. Switching to particles which are rigid as opposed to rubbery, the G_{IC} improvement is found to be at the most incremental [6, 11, 13]. Under Mode II fracture, nevertheless, it is common to observe a more significant and consistent G_{IIC} improvement [3, 5, 9, 10]. At this stage, however, it is still uncertain why the toughening effect due to the rubber particles is so different from that of rigid polymer modification. Detailed microscopic failure mechanisms studies on both systems, as will be described in this work, are needed for better understanding of the above uncertainties.

The present work, which is part of a larger effort that attempts to understand and improve composite CAI strength, focused on investigating the Mode I and Mode II delamination toughening mechanisms of TACTIX* 556 epoxy resin/AS4 fibre composite systems modified with either core–shell rubber (CSR) [19, 22, 23] or Proteus™ 5025 particles (B. F. Goodrich Company). The CSR particle has a uniform particle size of 0.1 μm, while the Proteus particle has an average particle size of about 20 μm. Because the particle sizes of the two modifiers are very different, the thicknesses of the interlaminar regions in the two rubber-modified composites are expected to be different. This allows the investigation of the effects of the interlaminar thickness and big particles on G_{IC}, G_{IIC} and CAI properties.

In order to observe the crack evolution process and the role the toughening particles play, the partially delaminated composites damage zones were analysed using optical microscopy (OM), scanning electron microscopy (SEM), and newly developed transmission electron microscopy (TEM) techniques [24]. In particular, the newly developed TEM technique, which requires extreme care in thin section preparation, enables us to study definitively how the composites fail and to understand the exact role of the toughener particles in the toughening process. Based on the findings, approaches for improving the G_{IC}, G_{IIC} and CAI of the toughened composites are discussed.

2. Experimental procedure

Composite laminates were fabricated by hand lay-up of unidirectional Hercules AS-4G fibre prepregged tapes based on a hydrocarbon epoxy novolac resin (i.e. TACTIX 556 epoxy resin) cured with 4,4′-diaminodiphenylsulphone (DDS). Unidirectional 24-ply and quasi-isotropic 32-ply $[45°, 0°, -45°, 90°]_{4S}$ laminates were fabricated for the delamination (i.e. both G_{IC} and G_{IIC} fracture toughness) and the CAI tests, respectively. A strip of fluorinated release film (12 μm thick) was inserted at the mid-plane of the laminates to act as a crack starter for the delamination tests. All panels were cured at 177 °C for 3 h and post-cured for 2 h at 238 °C. Laminates has fibre volume fractions ranging from 60%–64%. An ultrasonic C-scan was conducted to detect the void content of the laminates. Only panels with void volume fraction less than 3% were utilized.

The preformed CSR (0.1 μm) and Proteus™ 5025 ($\approx$ 20 μm) particles were used to toughen the epoxy composite. The epoxy matrix was mixed separately with 10 wt % CSR and 5 wt % Proteus particle tougheners prior to the prepregging process. The CSR particles, having a shell composition of styrene: methylmethacrylate: acrylonitrile: glycidylmethacrylate = 30:30:25:15, were found to disperse randomly in the epoxy matrix with adequate mixing and curing [23]. Therefore, this type of CSR particle has a viable chance to disperse randomly in the composite matrix and penetrate into the intralaminar region of the composite panel. For the Proteus particle-toughened composite, because the size of the Proteus particle ($\approx$ 20 μm) is much greater than the interfibre spacing ($\approx$ 0.2 μm) of the fibre bundles in each ply, the Proteus particles are expected to be filtered out by the fibre bundles and stay in the interlaminar region during the resin impregnation and composite consolidation processes. As a result, for the Proteus particle-modified composite system, the spacing in the interlaminar region (i.e. the thickness of the resin-rich interlaminar region) is expected to be comparable to the size of the Proteus particle. The effect of the thickness of the resin-rich interlaminar region in CAI strength improvement can thus be studied using these model epoxy composite systems.

* Trademark of The Dow Chemical Company.

Delamination tests were conducted by following the specimen definitions of recent ASTM round robins on end notch flexure (ENF) and double cantilever beam (DCB) tests of laminates. To ensure a sharp starter crack, a Mode I precrack was introduced prior to the (ENF) Mode II tests. The specimens were assumed to behave in accordance with the linear elastic beam theory during testing. Details of the testing procedures are described elsewhere by Friedrich [25] and Williams and co-workers [26–28]. Only crack initiation values of both the Mode I and Mode II delamination tests were reported. The CAI tests were conducted using a Dynatup 8250 instrumented impact tester with a 6.675 kJ m^{-1} impact energy set-up on the 10.2 cm × 15.2 cm panels specified by SACMA [29]. A steel base was used for the CAI tests.

In the microscopic investigations, the crack-tip region of the damaged specimens was cut into two halves at the mid-plane (core region), in a direction parallel to the fibre direction but perpendicular to the fracture surface. One-half of the specimen on the mid-plane was cut and polished using 0.3 μm alumina powder suspension for both OM and SEM investigations; the other half of the specimen was prepared for TEM study.

As part of the OM/SEM sample preparation, osmium tetraoxide (OsO_4) vapour was used for 16 h to stain the Proteus particle-modified composite. This helped induce sufficient phase contrast between the Proteus rubber and the matrix on the polished surface for both OM and SEM observations. The detailed experimental procedures for preparing the TEM thin sections are described elsewhere [23] but a brief description is given here. The crack-tip damage zones of the DCB and ENF CSR-toughened composite specimens were first isolated using OM and trimmed to a size of about 2 mm × 2 mm. The trimmed specimen was then embedded in a flat embedding mould, followed by further trimming, facing-off (Fig. 1), staining, and thin sectioning procedures. The ultra-thin sections were cut using a Reichert-Jung Ultracut E microtome with a diamond knife. They were placed on

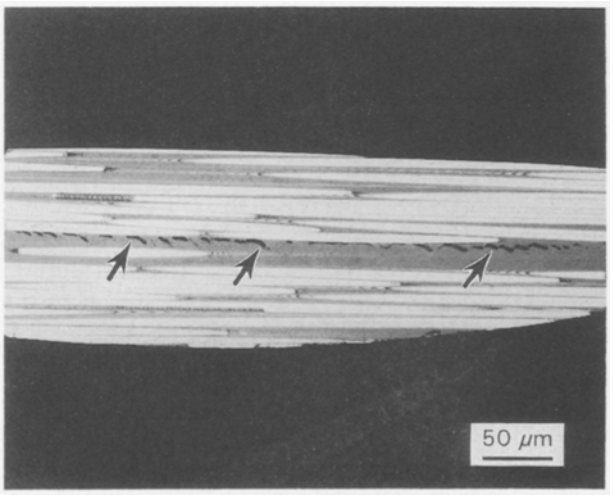

Figure 1 An optical micrograph of the CSR-modified composite showing the faced-off composite block. The shear cracks, indicated by the arrows, can be easily observed in the damage zone.

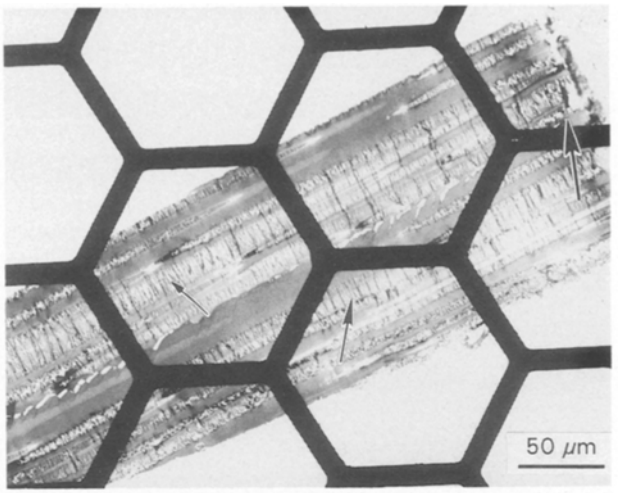

Figure 2 Transmission electron micrograph of the CSR-modified composite showing the integrity of the ultrathin section. The small arrows indicate the graphite phase. The large arrow indicates the Mode II crack tip.

200-mesh formvar-coated copper grids (Fig. 2) and examined using a Jeol 2000FX ATEM operated at an accelerating voltage of 100 kV. It is noted that the thin sectioning and isolation of the composite crack-tip damage zone for TEM observations is a delicate art. Extreme care must be taken to avoid causing damage to the thin section. Further, the thin sectioning direction must be made either parallel or at a small angle to the fibre direction to ensure the integrity of the fibres, and therefore, the integrity of the thin sections (Figs 1 and 2).

3. Results and discussion

3.1. Core–shell rubber-modified composite

Because of the small size of the CSR particles (≈ 0.1 μm), the role of these particles in the toughening of the composite cannot be clearly identified using either OM or SEM. Typical composite Mode I fracture surface features, using SEM, are shown in Fig. 3. Only information concerning the fibre/matrix charactersitics and the well-dispersed holes generated by the CSR particles can be obtained from these scanning electron micrographs. Information concerning the role of the rubber particles and the sequence of failure events during the toughening process cannot be learned from fracture surface study alone. Therefore, the newly developed TEM technique [24] is used to study the morphology and fracture behaviour of this composite.

3.1.1. Mode I fracture

The dispersion of the CSR particles in the composite panel is found to be excellent; no signs of agglomeration or trapping of the particles by the fibre bundles are found (Figs 4–15). Even in regions where fibre spacing is close to the size of the CSR particles, the CSR particles are still present (Fig. 4). This suggests that the CSR particles are so stable in the epoxy matrix that they flow freely with the resin during the

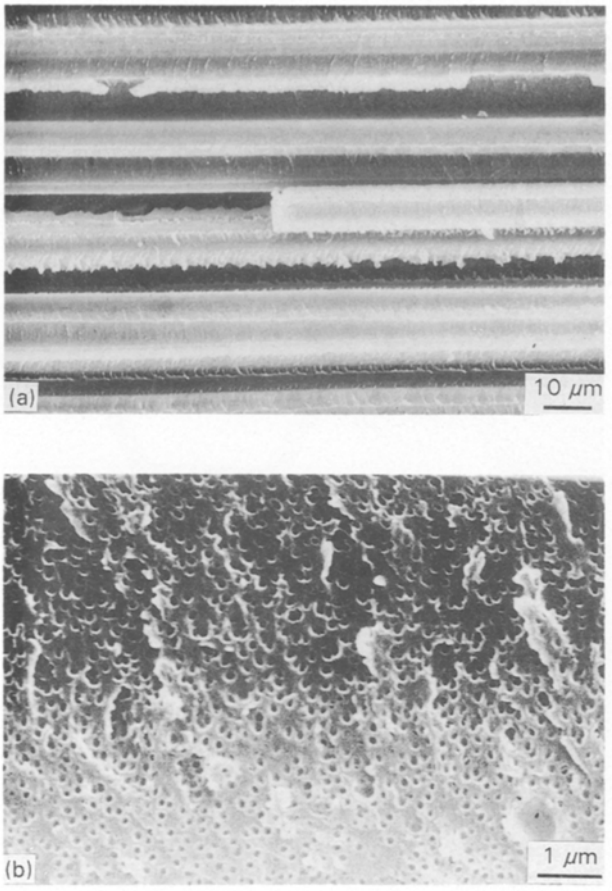

Figure 3 Typical Scanning electron micrographs of the CSR-modified composite showing the composite fracture surface features. (a) The fibre/matrix interfacial adhesion is seen to be quite good. (b) Well-dispersed holes found in the matrix. The crack propagates from right to left.

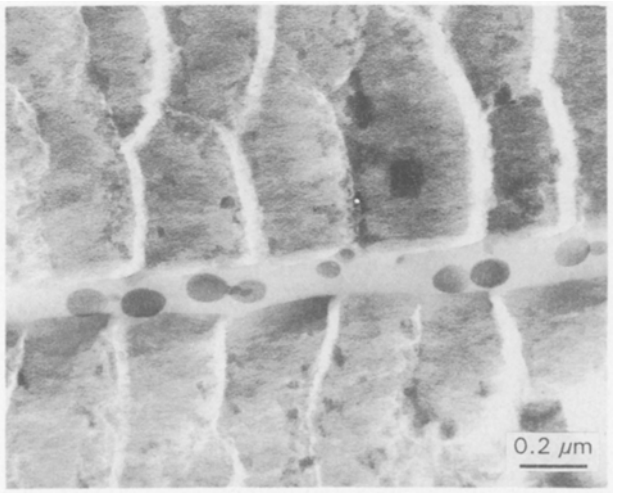

Figure 4 Transmission electron micrograph of the CSR-modified composite showing good penetration of the CSR particles into the fibre bundles.

prepregging and final moulding processes. Consequently, this specific type of CSR particle is highly suitable for applications where both interlaminar and intralaminar toughening of the high-performance epoxy composites are important [6, 19, 20, 30, 31].

The fracture behaviour of the CSR-modified composite under Mode I fracture is quite straightforward.

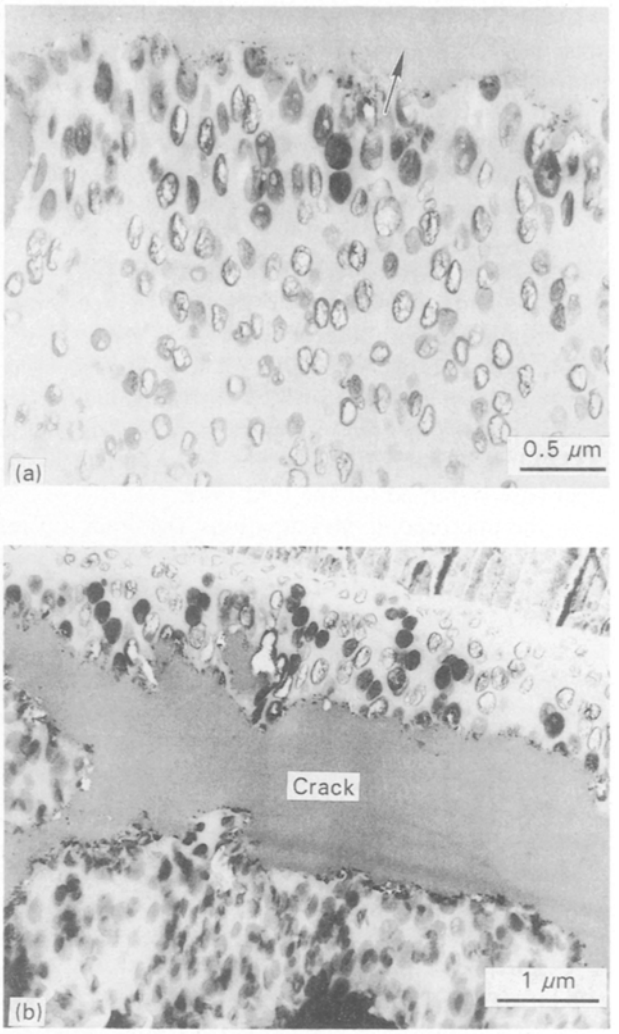

Figure 5 Transmission electron micrographs of the CSR-modified composite showing the cavitation and elongation of the CSR particles at the crack wake. The arrow in (a) indicates the crack, while the arrow in (b) indicates the fibre phase. The crack propagates from right to left.

As shown in Fig. 5, the CSR particles have cavitated and highly elongated in the crack wake region. This indicates that the matrix surrounding the highly elongated rubber particles also plastically deformed to a similar degree ($\approx$ 100% plastic strain). This phenomenon is found to be comparable to that of the CSR-modified neat epoxy system previously investigated [32]. Thus, the dominant toughening mechanisms in this toughened composite system are found to be cavitation of the CSR particles, which relieves the constraint in front of the crack tip, followed by shear yielding of the matrix. At locations about 5 μm away from the crack plane, the amount of rubber cavitation diminishes dramatically (Fig. 6). In cases where the crack grows close to the fibre phase, the rubber particle cavitation zone extends less than 2 μm beyond the other side of the fibre phase (Fig. 7). This is a substantially smaller cavitation zone than that observed in the CSR-modified neat resin case, where a rubber particle cavitation zone of $\approx$ 25 μm is observed [32]. This implies, as has been pointed out by others [3, 20], that the fibres hinder the growth of the rubber cavitation zone, which, in turn, may limit the

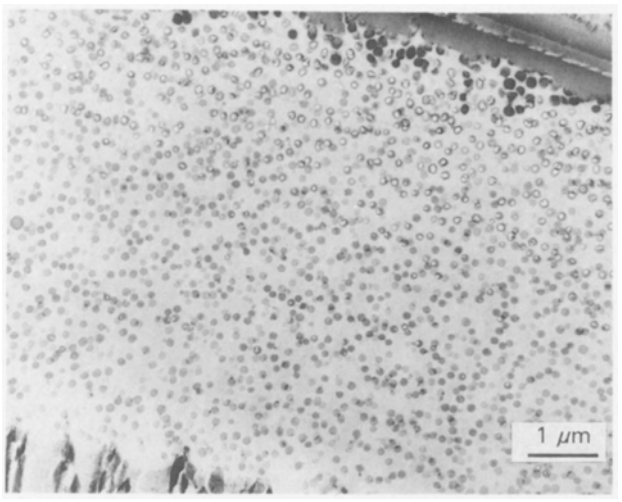

Figure 6 Transmission electron micrograph of the CSR-modified composite showing that the extension of the rubber cavitation zone is hindered by fibres. The upper right corner is the crack and the lower left corner is the fibre. The crack propagates from right to left.

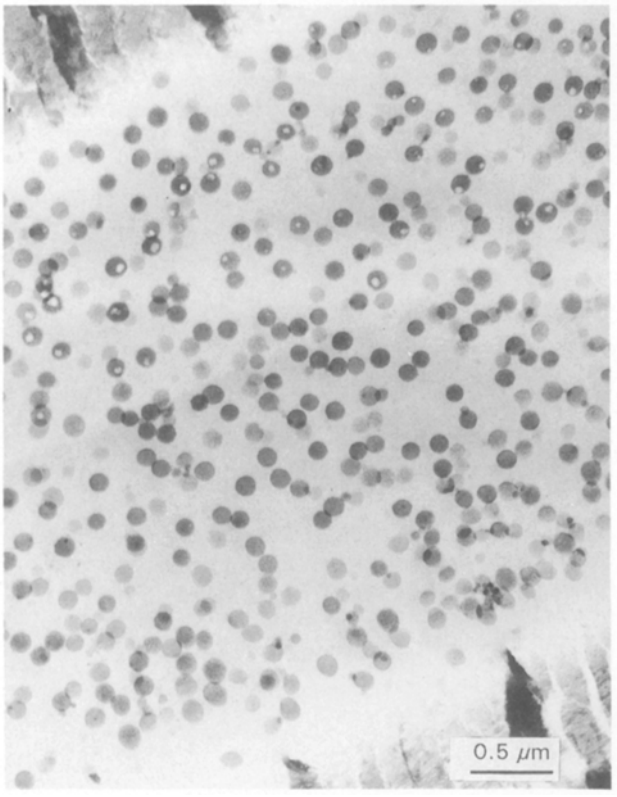

Figure 7 Transmission electron micrograph of the CSR-modified composite taken at a fibre spacing away from the crack wake. Very limited rubber cavitation is observed. The upper left and lower right corners are the fibre phase. The crack is located ≈ 1 μm above the upper graphite fibre.

volume of shear yielding material around the crack tip. This may partly explain the inability of rubber modification to give the expected toughening effect observed for some rubber-modified composites [2, 3, 6]. The CSR-modified composite system investigated in this study does, however, exhibit a significant toughening effect when tested using Mode I conditions (Table I). Over 200% improvement in G_{IC} is measured. The apparent inconsistency between the good G_{IC} values measured and the small damage zone size observed above can be rationalized as follows: (i) the size of the matrix crack tip shear yielded/banded zone is smaller than the thickness of the resin-rich interlaminar region [3, 20, 32, 33], (ii) the additional constraint imposed by the neighbouring fibres which induces a higher maximum principle stress, component around the crack-tip region produces a longer crack-tip plastic zone [33], and (iii) the fibre bridging mechanism takes place.

3.1.2. Mixed-mode and Mode II fractures

Hackles are one of the dominant features observed on the fracture surface of the unidirectional continuous fibre composites (Fig. 8), especially when the stress state is dominated by shear. Disputes over how the hackles are initiated and propagated are still unsettled [34–37]. In order to investigate unambiguously how the hackles form in the toughened composites, observation of the Mode II dominant crack-tip damage zone using an appropriate microscopic tool, i.e. the newly developed TEM technique, is needed.

To illustrate the development of hackle formation, a series of TEM micrographs are taken and are shown here. As shown in Fig. 9, a thin section taken at a location ≈ 2 mm below the thin sections investigated above (Figs 4–7) indicates the presence of significant mixed-mode failure [38]. At the crack-tip region, the hackle is formed from the existing shear cracks in front

TABLE I Fracture toughness and CAI strength of unmodified and modified model composites

	T_g (°C)	$G_{IC,\,ini.}$ (J m^{-2})	G_{IIC} (J m^{-2})	CAI (MPa)
Tactix*556/AS-4G	230	343	768	184
Tactix 556/AS-4G/10% CSR	215	825	664	234
Tactix 556/AS-4G/5% Proteus	225	492	942	196

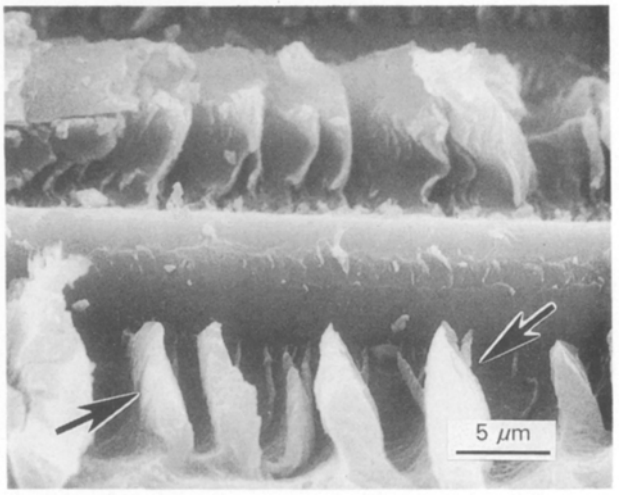

Figure 8 Scanning electron micrograph of the CSR-modified composite showing the hackles (see arrows). The crack propagates from right to left.

of the crack tip inside the resin-rich interlaminar region (Fig. 10). The investigation at the shear crack tip suggests that the shear cracks are initiated from the highly cavitated CSR particles (Fig. 11), which help trigger the initiation of the shear cracks along the maximum shear planes. When the neighbouring shear cracks grow close, they interact and cause reversed angle shear cracks to form (Fig. 12). The formation of the reverse angle shear cracks (Figs 12–14 and 16) may also be caused by the conjugated shear-stress component induced by the geometric restraint to offset the previously formed crack-tip shear cracks [39], in addition to the possible overlapping of the stress fields between the two neighbouring shear cracks. The main crack will then interact and link with these shear cracks, resulting in the formation of hackles (Fig. 13).

To support further the above description of the evolution of hackles, the fracture behaviour of the

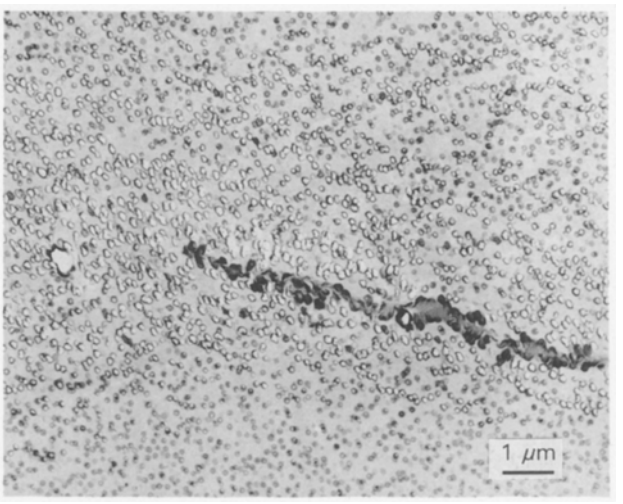

Figure 11 Transmission electron micrograph of the CSR-modified composite showing the tip of the shear crack in front of the crack tip. It is evident that the CSR particles are highly cavitated and elongated around the shear crack. The crack propagates from right to left.

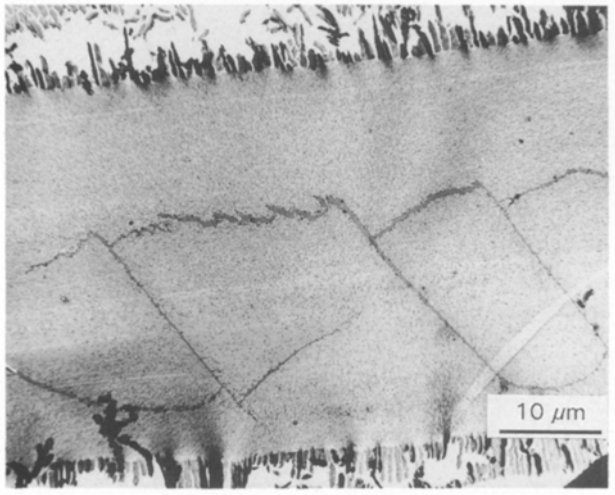

Figure 9 Transmission electron micrograph of the CSR-modified composite showing the hackles, viewed on the plane parallel to the crack direction but perpendicular to the fracture surface, in the crack wake region. The top and bottom are the fibres. The crack propagates from right to left.

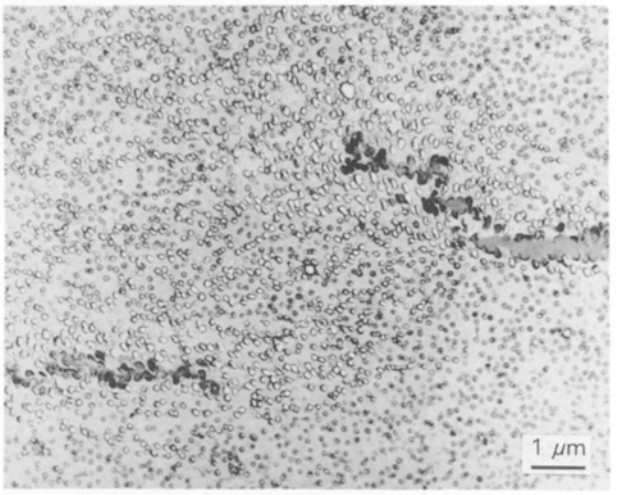

Figure 12 Transmission electron micrograph of the CSR-modified composite showing the interaction of two neighbouring shear cracks. The matrix between the two shear cracks appears to have deformed to a higher degree, compared to the surrounding matrix. The crack propagates from right to left.

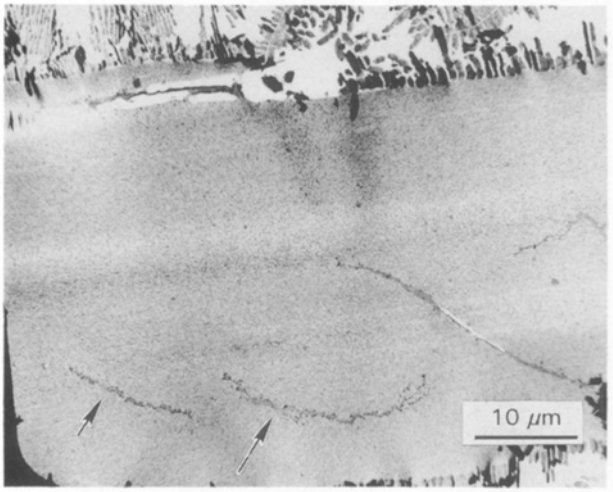

Figure 10 Transmission electron micrograph of the CSR-modified composite showing the formation of shear cracks (see arrows) in front of the crack tip. The top and bottom are the fibres. The crack propagates from right to left.

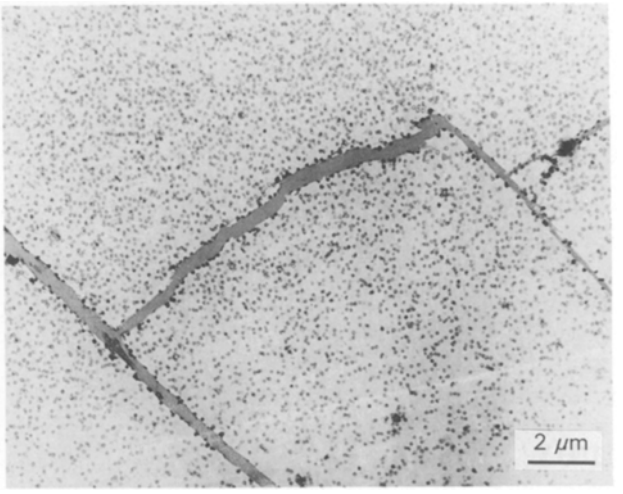

Figure 13 Transmission electron micrograph of the CSR-modified composite showing the formation of hackles. The crack propagates from right to left.

same composite tested under ENF Mode II testing was investigated. At the sub-surface of the ENF fracture surface, viewed using TEM, it was found that, as expected, the edges of the hackles were aligned at nearly a 45° angle with respect to the fibre direction (Fig. 14). The formation of the hackles was again found to be initiated from the toughener particles inside the resin-rich region, not at the fibre/matrix interface. The initiation of the shear cracks appears to be due to the shear-induced cavitation of the CSR particles (Fig. 15). When the weak shear plane due to the cavitated CSR particles is established, the shear crack will then form ahead of the crack tip. The opposite angle shear cracks are then formed due to both the dominant Mode II loading and the interaction of the adjacent shear cracks. This observation is in agreement with the explanation given above. The mechanisms for the formation of hackles are summarized in Fig. 16.

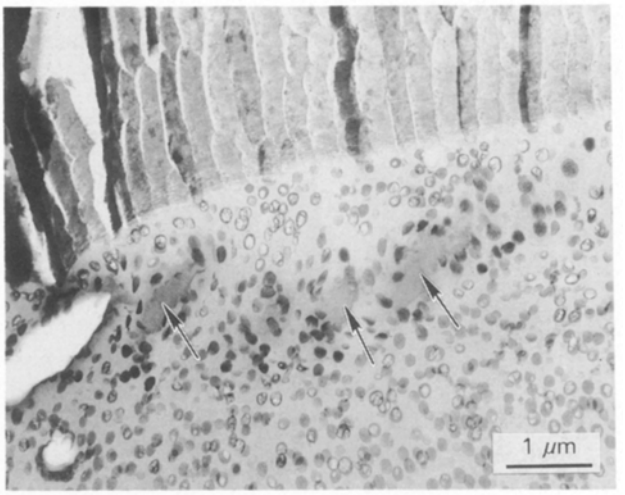

Figure 15 Transmission electron micrograph of the ENF sub-surface damage zone of the CSR-modified composite showing the initiation (see arrows) of the shear cracks due to the CSR particles. The top is the fibre phase. The crack propagates from right to left.

3.2. Proteus particle-modified composite

As the size of the Proteus particles is ≈ 20 μm, both OM and SEM will provide sufficient resolution for the investigation of the morphology and the failure mechanisms in this modified composite system. The TEM investigation, which is both costly and time consuming, is not needed.

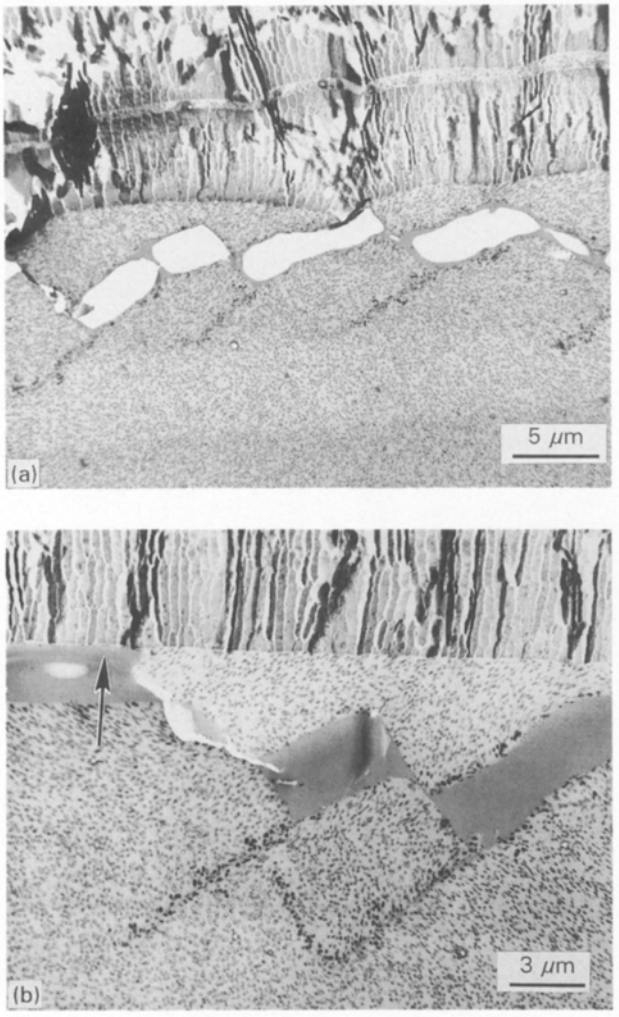

Figure 14 Transmission electron micrograph of the ENF sub-surface damage zone of the CSR-modified composite showing hackles. As shown in (a), it is clear that the majority of the hackles form and grow inside the resin-rich interlaminar region. In (b), occasional interfacial failure (see arrow) takes place as a result of the overgrown shear crack. The crack propagates from right to left.

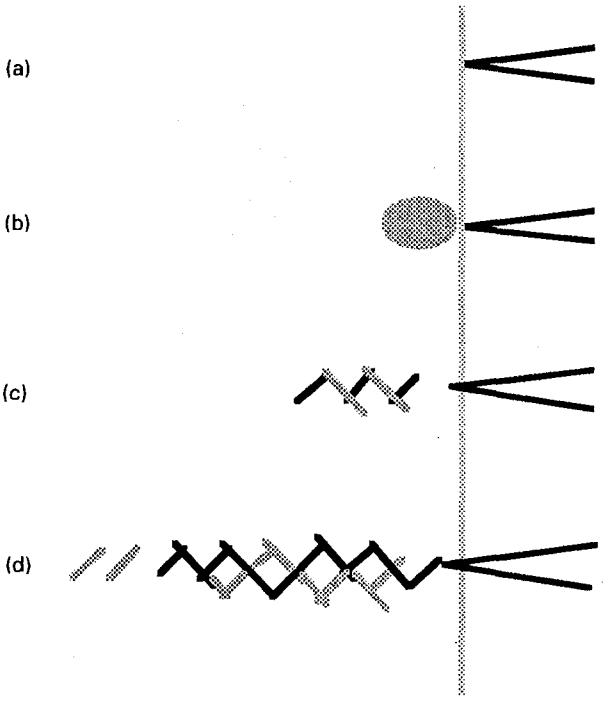

Figure 16 Summary of the evolution of the hackle formation. (a) A starter crack, (b) shear yielding and cavitation of the rubber particles in front of the crack tip is induced by Mode II loading, (c) shear cracks begin to form, (d) the interaction of the neighbouring shear cracks as well as the Mode II dominant stress cause the reverse shear cracks to form. Therefore, the hackles become apparent after the main crack propagates through them.

3.2.1. Mode I fracture

The Proteus particles, which appear to be partially swollen by the epoxy matrix [19], are found to be randomly dispersed in the interlaminar region, as can be expected from the large size of the particles. Although in some locations, the Proteus particles either

merge with adjacent particles or disintegrate into irregular domains (as described in the following), the Proteus particles still provide approximately the same spacing within the laminate. The thickness of the interlaminar resin-rich region ranges from about 30–100 μm (Fig. 17). The comparison between the CSR and the Proteus particle-modified composites will allow a more definitive understanding of the effect of ply spacing on the mechanical performance of the composites.

Reflected Nomarski OM was utilized to study the sub-surface damage zone prepared parallel to the fibre direction and perpendicular to the fracture surface from the mid-plane core region. The fracture behaviour of this toughened composite system is found to be similar to that of the Proteus particle-modified neat epoxy system [32]. Under Mode I testing, the crack appears to grow unperturbed through the particles. Occasional crack-deflection and crack-bifurcation mechanisms are found (Fig. 18). These toughening mechanisms have been shown to be less effective than those which involve plastic shear flow of the epoxy matrix [32]. Only an incremental toughening effect is found in this composite system (Table I). In other words, the restraints induced by the sharp crack and the presence of the fibre phase cannot be relieved by the Proteus particle modification; no apparent matrix plastic deformation is observed when the composite is subject to Mode I delamination.

3.2.2. Mode II fracture

Under Mode II fracture, the Proteus particles appear to play a more significant role in the toughening process. Significant amount of hackles are found everywhere on the fracture surface, due to the thick layer of the interlaminar resin-rich region (Fig. 19). Careful observations on the entire fracture surface indicate that only at some isolated areas are the fibres observed on the fracture surface (Fig. 20). This implies that the majority of the hackles form within the interlaminar resin-rich region.

When the damage zone is studied and viewed in a direction parallel to the fibre direction and perpendicular to the fracture surface, the sequence of events leading to the formation of hackles can be more clearly understood. The spacing and location of the hackles appear to be related to the presence of the Proteus particles. The shear cracks seem to be

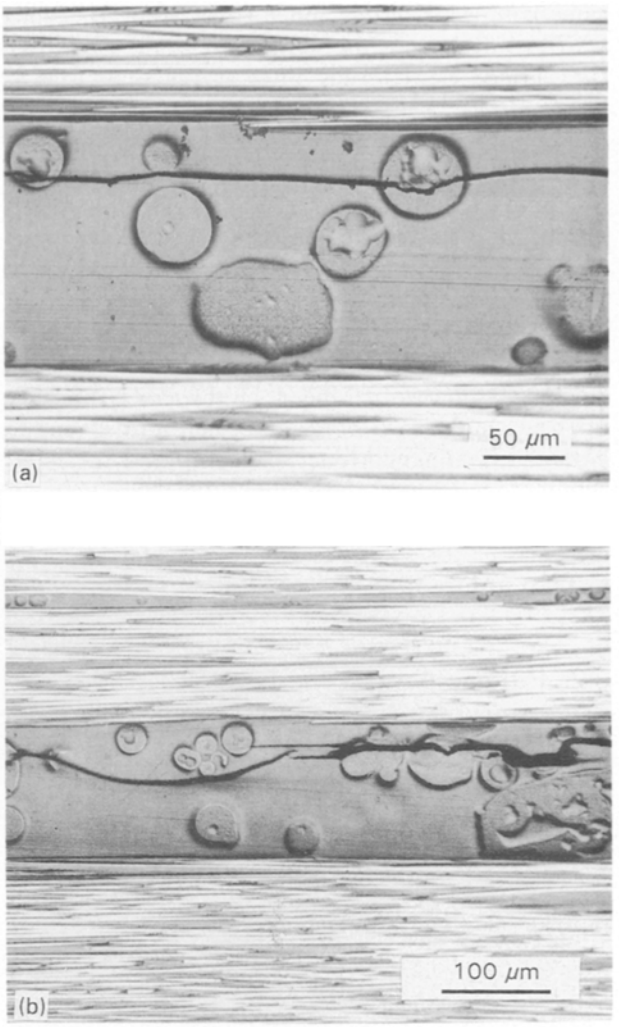

Figure 18 Reflected optical micrographs of the Proteus particle-modified composite showing that under Mode I failure, only (a) crack deflection and (b) crack bifurcation mechanisms are found. The crack propagates from right to left.

Figure 19 Scanning electron micrograph showing the fracture surface of the Proteus particle-modified composite. The majority of the fracture surface is covered by the epoxy matrix due to the thick layer of the interlaminar resin-rich region. The arrow indicates a Proteus particle. The crack propagates from right to left.

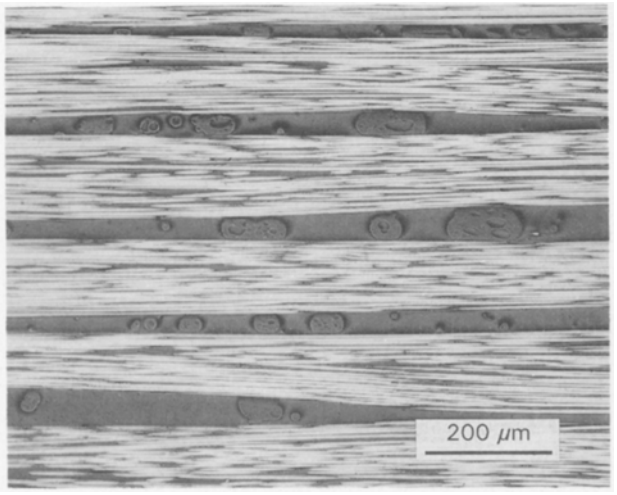

Figure 17 An optical micrograph showing the interlaminar spacing between plies of the Proteus particle-modified composite.

initiated at either the interface between the matrix and the particle or the interior of the Proteus particles. The shear cracks then extend toward the fibre/matrix interface (Figs 21 and 22). These fibre/matrix interfacial cracks will either grow toward the resin-rich region and interact with the pre-existing shear cracks or simply stop growing at the interface (see arrows in Figs 21 and 22). This phenomenon again supports the proposed process mentioned in the CSR-modified composite system above for the formation of hackles in toughened composites.

The G_{IC} improvement of the CSR-modified composite is much greater than that due to the Proteus particle modification (Table I). Even though the Proteus particles produce a significantly larger resin-rich region for the matrix fully to deform plastically without the fibre constraint, the CSR particles, which cavitate and help promote extensive plastic shear flow of the epoxy matrix, appear to be more effective in toughening the high-performance composites. This implies that in order for the G_{IC} improvement in the composite to be effective, the toughener particles need to act as (i) constraint relievers and (ii) stress concentrators, as in the case of the rubber-modified neat epoxy system [20, 32]. Furthermore, because the size of the shear-yielded zone can be limited by the surrounding fibres, any toughening mechanisms that involve the fracture surface, such as crack/particle bridging, crack-bifurcation, and crack-deflection, should be promoted, if G_{IC} is to be further increased. This idea is supported by our earlier studies on a series of model CSR-modified epoxy system [23]. In those model systems studies, it was found that both rubber cavitation/matrix shear yielding mechanisms and the crack deflection mechanism can operate simultaneously during fracture, as long as the dispersion of the CSR particles in the epoxy matrix is adequately controlled. The G_{IC} can jump from the unmodified epoxy value of 180 J m^{-2}, to 490 J m^{-2} for the case where only rubber cavitation/matrix shear yielding mechanisms operate, and to 640 J m^{-2} for the concurrent operations of both rubber cavitation/matrix shear yielding and crack-deflection mechanisms.

Figure 20 Scanning electron micrograph showing the fracture surface of the Proteus particle-modified composite. The arrow indicates a Proteus particle. The crack propagates from right to left.

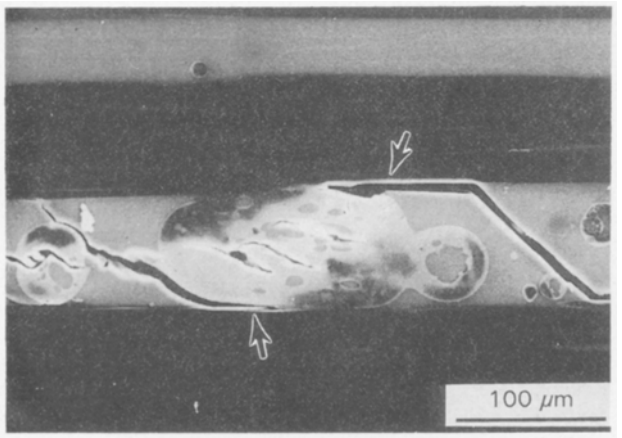

Figure 21 Scanning electron micrograph showing the sub-surface damage zone of the Proteus particle-modified composite. The arrows indicate the stopped interfacial cracks. The crack propagates from right to left.

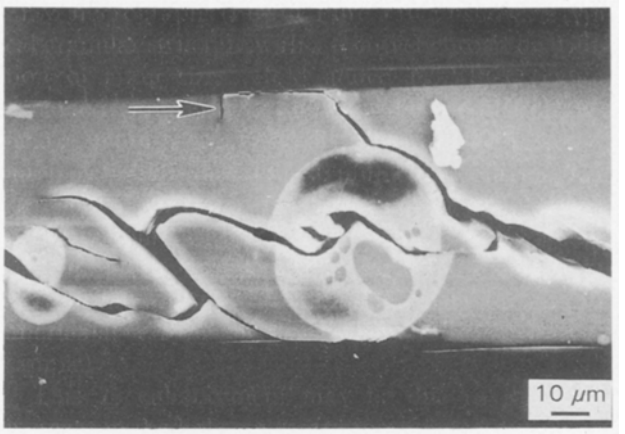

Figure 22 Scanning electron micrograph showing the sub-surface damage zone of the Proteus particle-modified composite. The arrow indicates turning of the interfacial crack toward the resin-rich region. The crack propagates from right to left.

Under Mode II fracture, Bradley and co-workers [4, 9, 40] have extensively studied and correlated the G_{IIC} of the composites with the hackle patterns on the composite fracture surface. They state that the tougher is the matrix, the larger will be the hackle spacing. When the matrix is extremely tough, the hackle pattern disappears. In the case of toughened composites, based on the present work, the formation of the shear cracks, which appear to be the precursor for the hackle formation, is facilitated by the presence of the toughener particles. As a result, the size and spacing of hackles will be affected by both the size and concentration of the toughener particles in the matrix, in addition to the ductility of the matrix material as proposed by Hibbs and Bradley [40]. Thus, care should be taken if the toughening effect is to be correlated with the hackle patterns observed on the composite fracture surface.

The Mode II toughening is found to be more effective for the Proteus particle-modified system than for the CSR-modified system (Table I). Because the CSR particles have about two to three orders of magnitude lower elastic modulus than that of the epoxy matrix, the level of stress intensification [16] around the toughener particles due to the CSR is

much higher than that due to the Proteus particle (a rather rigid particle with a T_g of 28 °C [32]). The stress magnitude required to cavitate the CSR particles is also found to be much lower than that for the Proteus particles [32]. As a result, the energy needed to cause the shear cracks to form and grow in the CSR-modified composite is much lower than that for the Proteus particle-modified epoxy composite. Therefore, attempts to improve the G_{IIC} of the composite should involve the utilization of a toughener particle that possesses cavitational strength and elastic constants (e.g. Young's modulus and Poisson's ratio) close to those of the epoxy matrix. If rubber particles are to be used for an overall balance of properties, the amount of rubber particles to be incorporated should be minimized to avoid significant stress overlap, which will further decrease the G_{IIC} of the composite. We therefore surmise that the low stress concentration factor as well as the effective creation of the crack-tip damage zone are the two main causes for the effective Mode II toughening via thermoplastic modification over those via rubber modification [6, 11].

It is noted that even though Proteus particles are partially swollen by the epoxy matrix, mechanically they still behave differently from the epoxy matrix and can still effectively trigger the formation of hackles. It is also noticed that even though hackles are formed due to the dominance of the Mode II loading, the amount of shear yielding in the matrix may not always be significant. As indicated in Figs 13 and 23, very limited matrix shearing, if any at all, is observed on the hackled regions. This suggests that the observation of hackles does not directly indicate the presence of significant matrix shear yielding.

The occasional debonding at the fibre/matrix interface observed on the fracture surface of toughened composites in the present study (Figs 8 and 20) appears to be due to the overgrowth of the shear cracks into the fibre/matrix interface (Figs 14, 21 and 22). Because the majority of the shear cracks form inside the resin-rich interlaminar region, the main crack grows predominantly inside the resin-rich region. Therefore, the interfacial adhesion between the fibre and matrix should be adequate. No additional effort is needed to improve the interfacial adhesion for the toughened composite systems investigated here. Also, it is evident that, based on the present work, any experiments solely involving fracture surface investigations can lead to erroneous conclusions. In other words, care should be exercised when descriptions of the damage evolution are largely based on fracture surface observations. To elucidate this point, a schematic illustration of how the fracture surface investigation can sometimes lead to the conclusion that the hackles are initiated from the fibre/matrix interface is shown in Fig. 24. The present study has clearly proven otherwise.

Although damage analyses of both partially and fully damaged CAI panels are still subject to future investigations, the present work has provided an important insight concerning the approach for improving the CAI strength of high-performance composites. The use of the Proteus particles to generate thick resin-rich interlaminar layers does not produce any significant improvement in composite CAI strength (Table I). This implies that a thick layer resin-rich interlaminar region does not guarantee an improved CAI strength of the composite. Therefore, it is possible that the type of toughener particles utilized is also as important as, if not more important than, the thick-layer interlaminar resin-rich region. This conjecture is to be verified from future investigations. Furthermore, as shown in Table I, the improvement of the composite G_{IIC} via the Proteus particle modification does not ensure any sizable improvement of the composite CAI strength. Conversely, a drop in the composite G_{IIC} due to CSR modification does not result in any loss in the composite CAI strength. Instead, the significant improvement of G_{IC} via the CSR modification does produce a moderate composite CAI strength enhancement. Consequently, any sole emphasis of the importance of the G_{IIC} toughness as a guideline for composite CAI strength is bound to oversimplify the nature of the composite CAI behaviour. For example, the intralaminar toughness of the composite may be as critical as the delamination fracture toughnesses.

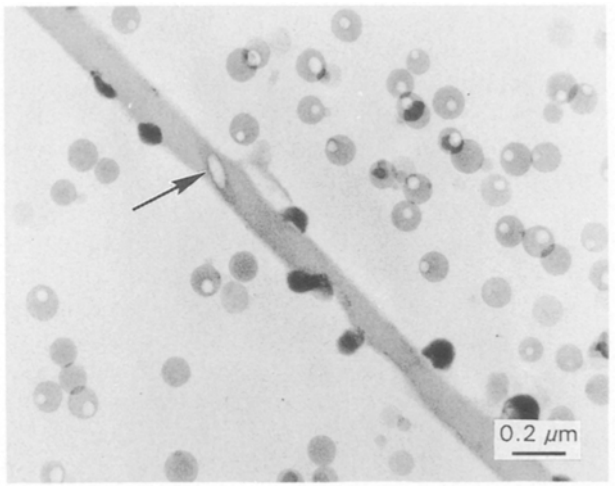

Figure 23 Transmission electron micrograph of the CSR-modified composite showing that the degree of shear in the shear plane is extremely high (see the shearing of the CSR particles on the shear plane shown by the arrow). However, except for the cavitation of the CSR particles, the matrix immediately beneath the shear plane is undeformed.

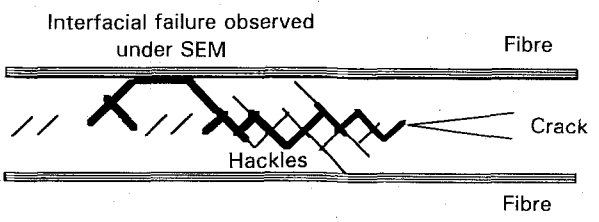

Figure 24 A schematic illustration of the growth of the hackle with respect to the surrounding fibre/matrix interface under Mode II shear. It is evident that observations based on the fracture surface study can sometimes be misleading. The apparent debonding at the interface (Fig. 8) may very well be due to the overgrowth of the shear cracks, which is originated from the toughener particles inside the resin-rich region of the composite. The dark lines indicate the route of the main crack when it grows.

Clarifications of the above concerns will rely on future investigations of model composite systems.

4. Conclusion

It has been found that the newly developed TEM technique is extremely useful for both morphology and failure mechanisms studies of toughened composites. The CSR particles were found to disperse randomly in the epoxy composite. The failure mechanisms in the model toughened composites, under Mode I fracture, were found to be similar to those of the neat rubber-modified epoxy systems. Under a Mode II dominant stress field, the major failure feature is the formation of hackles. It is unambiguously shown that the hackles in the toughened composites are initated from the toughener particles inside the resin-rich interlaminar region, not at the fibre–matrix interface. The use of rigid polymers is recommended for Mode II toughening of high performance composites. The CAI strength appears to be related to the type of interleaving particles, in addition to the thickness of the interlaminar resin-rich region, the G_{IC} and G_{IIC} delamination toughnesses, and possibly, the intralaminar toughness of the composite.

Acknowledgements

The authors thank D. L. Barron, N. A. Orchard, D. M. Pickelman, P. C. Yang, C. C. Garrison, P. M. Puckett, B. L. Burton, E. T. Vreeland, and R. D. Peffley for their valuable discussion, experimental assistance and support of this work.

References

1. N. ODAGIRI and H. KISHI, *Polym. Preprint* **33** (1992) 384.
2. D. S. PARKER and A. F. YEE, *J. Therm. Compos. Mater.* **2** (January) (1989) 2.
3. W. L. BRADLEY, in "Application of Fracture Mechanics to Composite Materials", edited by K. Friedrich (Elsevier Applied Science, New York, 1989) p. 159.
4. C. R. CORLETO and W. L. BRADLEY, in "Composite Materials: Fracture and Fatigue", Vol. 2, ASTM STP 1012, edited by P. A. Lagace (American Society for Testing and Materials, Philadelphia, PA, 1989) p. 201.
5. C. B. BUCKNALL, in "Advanced Composites", edited by I. K. Partridge, (Elsevier Applied Science, New York, 1989) p. 145.
6. D. L. CRANE, MS thesis, Texas A and M University (1990).
7. W. L. BRADLEY, in "Proceedings of the Benibana International Symposium", October 1990.
8. D. HUNSTON and R. DEHL, "The Role of Matrix Toughness in Matrix Dominated Composite Fracture" (Society of Manufacturing Engineers, 1987) p. 355.
9. W. L. BRADLEY, in "The Role of Matrix Properties on the Toughness of Thermoplastic Composite", edited by R. B. Pipe (Elsevier Applied Science, New York, 1991) p. 295.
10. J. E. MASTERS, in "Proceedings of 6th International Conference on Composite Materials", Vol. 3 (Elsevier Applied Science, New York, 1987) p. 396.
11. I. GAWIN, US Pat. 4783 506 (1988).
12. R. E. EVANS, and K. R. HIRSCHBUEHLER, US Pat. 4604 319 (1986).
13. N. ODAGIRI, H. KISHI and T. NAKAE, "T800H/3900-2 Toughened Epoxy Prepreg System: Toughening Concept and Mechanism" (6th American Society for Composites, New York, 1991) p. 43.
14. M. A. HOISINGTON and J. C. SEFERIS, "Process-Structure-Property Relationship for Layered Structured Composites" (6th American Society for Composites, New York, 1991) p. 53.
15. H.-J. SUE, R. A. PEARSON and A. F. YEE, *Polym. Eng. Sci.* **24** (1989) 1447.
16. H.-J. SUE, PhD thesis, The University of Michigan, Ann Arbor, MI (1988).
17. H.-J. SUE and A. F. YEE, *J. Mater. Sci.* **26** (1991) 3449.
18. K.-K. KOO, T. INOUE and K. MIYASAKA, *Polym. Eng. Sci.* **25** (1985) 741.
19. H.-J. SUE, E. I. GARCIA-MEITIN and P. C. YANG, *Composites* (1992) submitted.
20. A. F. YEE. in "Toughened Composites", STP 937, edited by N. J. Johnston (American Society for Testing and Materials, Philadelphia, PA, 1986) p. 383.
21. R. E. JONES and D. L. CALDWELL, "The Correlation of Resin Toughness and the Fiber-Resin Interfacial Shear Strength with Damage Tolerance" (5th American Society for Composites, New York, 1990) p. 154.
22. D. E. HENTON, D. M. PICKELMAN, C. B. ARENDS and V. E. MEYER, US Pat. 4778 851 (1988).
23. H.-J. SUE, E. I. GARCIA-MEITIN, D. M. PICKELMAN and P. C. YANG, in "Toughened Plastics: Science and Engineering", ACS Vol. 233, edited by C. K. Riew, in press.
24. E. I. GRACIA-MEITIN and H.-J. SUE, in preparation.
25. K. FRIEDRICH (Ed.), "Application of Fracture Mechancis to Composite Materials" (Elsevier Science, New York, 1989).
26. S. HASHEMI, A. J. KINLOCH and J. G. WILLIAMS, *Proc. R. Soc.* **A427** (1990) 173.
27. J. G. WILLIAMS, *J. Strain Anal.* **24** (1989) 207.
28. S. HASHEMI, A. J. KINLOCH and J. G. WILLIAMS, in "Composite Materials: Fatigue and Fracture", Vol. 2, ASTM STP 1110, edited by T. K. O'Brien (American Society for Testing and Materials, Philadelphia, PA, 1991) p. 143.
29. SACMA Standard SRM 2–88.
30. P. C. YANG, E. P. WOO, S. A. LAMAN, J. J. JAKUBOWSKI, D. M. PICKELMAN and H.-J. SUE, in "36th International SAMPE Conference", Vol. 36 (1991) p. 437.
31. A. J. LESSER and A. G. FILIPPOV, *ibid.* Vol. 36 (1991) p. 886.
32. H.-J. SUE, *Polym. Eng. Sci.* **31** (1991) 275.
33. A. J. KINLOCH, "Adhesion and Adhesives" (Chapman and Hall, New York, 1987).
34. W. D. BASCOM and S. Y. GWEON, in "Fractography and Failure Mechanisms in Polymers and composite", edited by A. C. Roulin-Moloney (Elsevier Applied Science, New York. 1989).
35. T. JOHANNESSON, P. SJOBLOM and R. SELDEN, *J. Mater. Sci.* **19** (1984) 1171.
36. G. E. MORRIS, in "Nondestructive Evaluation and Flaw Critically for Composite Materials", edited by R. B. Pipe, ASTM STP 696 (American Society for Testing and Materials, Philadelphia, PA, 1979) p. 274.
37. B. W. SMITH and R. A. GROVE, in "Fractography of Modern Engineering Materials", edited by J. E. Masters and J. J. Au, ASTM STP 948 (American Society for Testing and Materials, Philadelphia, PA, 1987) p. 154.
38. M. CHARALAMBIDES, A. J. KINLOCH, Y. WANG and J. G. WILLIAMS, *Int. J. Fract.* (1992) in press.
39. P. B. BOWDEN, in "The Physics of Glassy Polymers" edited by R. Haward (Applied Science, London, 1973).
40. M. F. HIBBS and W. L. BRADLEY, in "Fractography of Modern Engineering Materials", edited by J. E. Masters and J. J. Au, ASTM STP 948 (American Society for Testing and Materials, Philadelphia, PA, 1987) p. 68.

Received 20 July
and accepted 27 April 1993